Understanding water jet and metal stream interactions during water atomization of steel powders using analytical and CFD modeling techniques

Conference Paper · June 2017

CITATIONS
0

READS
773

8 authors, including:

Cheng-Tse Wu
University of Toronto
4 PUBLICATIONS **3** CITATIONS
SEE PROFILE

Ali Asgarian
University of Toronto
22 PUBLICATIONS **26** CITATIONS
SEE PROFILE

Saikat Chatterjee
M. N. Dastur & Company (P) Ltd.
39 PUBLICATIONS **94** CITATIONS
SEE PROFILE

Vlad Paserin
University of Waterloo
19 PUBLICATIONS **233** CITATIONS
SEE PROFILE

Understanding water jet and metal stream interactions during water atomization of steel powders using analytical and CFD modeling techniques

Cheng-Tse Wu[1], Ali Asgarian[2], Saikat Chatterjee[2], Bruno Girard[3], Vladimir Paserin[3], Francois Lavallee[3], Markus Bussmann[1], Kinnor Chattopadhyay[2]

1. Department of Mechanical and Industrial Engineering, University of Toronto, 5 King's College Road, Toronto, Ontario, Canada M5S 3G8
2. Department of Materials Science & Engineering, University of Toronto, 184 College Street, Toronto, Ontario, Canada M5S 3E4
3. Rio Tinto, Fer et Titane, 1625, route Marie-Victorin, Sorel-Tracy, Quebec, J3R 1M6, Canada

Abstract

Water atomization of metal powder is a process whereby a series of water jets impinging on a stream of liquid metal creates small droplets. As currently known to researchers, formation of metal droplets is affected by apex angle and molten metal properties, which in turn influence the final particle size distribution. However, manipulating and controlling the range of particle size distribution remains difficult in the industry. Therefore, the process from jet impingement to droplet formation was investigated using analytical methods and computational fluid dynamics simulations. A multiphase axisymmetric computational fluid dynamic (CFD) domain was developed to simulate the liquid metal stream-water jet interaction under various operating conditions. The breakup behavior was observed and explained by analyzing the influence of apex angle on water jet momentum transfer, total kinetic energy transfer, effect of surface energy, and vapor formation phenomenon.

1. Introduction:

For decades, high-pressure water atomization has been used for the production of various metal alloy powders and has been particularly applied for ferrous metal powders due to its high production capability. The process begins with tapping molten metal from ladle to a tundish. Subsequently, the molten metal flows through a ceramic nozzle located at the bottom of the tundish into the atomization system. The molten metal stream exiting the nozzle falls freely onto the crossflow of high-pressure water jets and disintegrates into fine metal particles [1] as shown in Fig.1. Depending on the market requirement the powder is sieved and classified by particle size. The efficacy of the water atomization process is predominantly evaluated based on particle size distribution of the atomized metal since only certain ranges of particle are deemed valuable to the market. At high production scale, a precise control of the size distribution would lead to the elimination of undesired particle size and an increase in production yield.

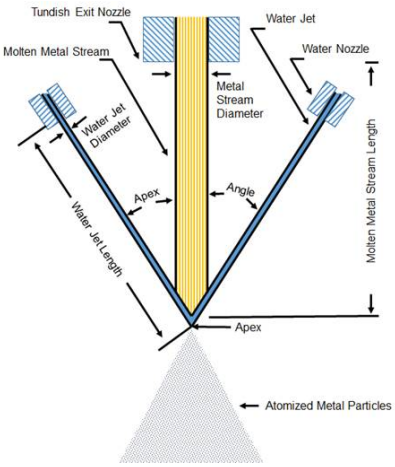

Figure 1. Illustration of water atomization process

The size distribution of the atomized metal particles depends on the interaction between the molten metal stream and the water jet during atomization. In the past, investigators have attempted to manipulate and predict the particle size distribution with various operational parameters, through experimental and mathematical studies.

Studies by Persson [2], Dunkley [3] and Bergquist [4,5] showed that, by raising superheat and changing the alloy composition of the molten metal, the resulting decrease in surface tension and viscosity leads to a narrower particle size distribution and reduced mass median particle size (d_{50}) of water-atomized metal powders. Persson [6] further emphasized the influence of the relationship of carbon and sulphur content in Fe-C-S alloys to surface tension and viscosity, which ultimately affects d_{50}.

Dhokey [7], Dunkley [3,8] and Grandzol [9] investigated the influence of apex angle on the mass median particle diameter of atomized metals. They concluded that increasing apex angle decreases d_{50}.

Although manipulating operation parameters to influence the particle size distribution has been extensively examined, the interaction between a molten metal stream and a water jet at macroscopic level is yet to be explored. In order to achieve precise control of the metal powder production process, it is necessary to understand the behavior of molten metal during water atomization.

Aller [10] proposed and illustrated the formation of steam pockets on the molten metal surface upon impact with water droplets. Yet, the cause of such behavior was unexplained. It is suspected that the formation of steam at the molten metal/water jet interface, as illustrated by Aller [10], may cause a violent phenomenon called a "vapor explosion".

The main objective of this work was to study the influence of various operational parameters on the interaction between a molten metal stream and a water jet during primary atomization. The intention of this study deviates from predicting the exact particle size distribution produced by various configurations. Computational fluid dynamics (CFD) modeling was implemented to investigate the breakup behavior of the molten metal stream at different apex angles. First and second sections of this paper focus on understanding momentum and kinetic energy transfer at various apex angles. In the third section, the study examines the influence of surface energy to the breakup of molten metal at primary and secondary atomization zones. Lastly, CFD was used to visualize the steam pocket formation at the molten metal/water jet interface.

2. CFD Modeling

This study was performed using the commercial CFD code, *ANSYS FLUENT 16.2*, using the Volume of Fluid (VOF) model coupled to the standard *k-ω* turbulence model. Evaporation model were used to study the interaction between the liquid metal stream and the water jet.

2.1 Mathematical models

Standard $k-\omega$ turbulence model

The standard $k-\omega$ model of Wilcox [11] was implemented in the CFD model to simulate jet flow-generated turbulence. The model solves a series of transport equations for *k*, the turbulence kinetic energy, and, *w*, the specific dissipation rate.

$$\frac{Dk}{Dt} = \Gamma_k \cdot \nabla^2 \cdot k + G_k - Y_k + S_k$$

$$\frac{D\omega}{Dt} = \Gamma_\omega \cdot \nabla^2 \cdot \omega + G_\omega - Y_\omega + S_\omega$$

where Γ_k and Γ_ω

$$\Gamma_k = \mu + \frac{\mu_t}{\sigma_k}, \Gamma_\omega = \mu + \frac{\mu_t}{\sigma_\omega}$$

$$\mu_t = \alpha^* \cdot \frac{\rho k}{\omega}$$

$$\alpha = \frac{\alpha_\infty}{\alpha^*}\left(\frac{\alpha_0 + Re_t/R_\omega}{1 + Re_t/R_\omega}\right)$$

where α is a coefficient defined to be equal to 1 in a system with high-Reynolds number.

$$G_k = -\rho\overline{u_i' u_j'}\frac{\partial u_j}{\partial x_i}$$

$$G_\omega = \alpha\frac{\omega}{k}G_k$$

$$Y_k = \rho\beta^* f_{\beta^*} kw$$

$$Y_\omega = \rho\beta f_\beta \omega^2$$

where the parameters G_k and G_ω depict the production of turbulent kinetic energy and specific dissipation rate respectively; Y_k and Y_ω depict the dissipation of *k* and *w* due to turbulence; S_k and S_ω are user-defined source terms. The values for the constants in the standard *k-ω* turbulence model recommended by Wilcox [11] are $\alpha_\infty^* = 1, \alpha_\infty = 0.52, \alpha_0 = \frac{1}{9}, R_k = 6, R_\omega = 2.95, \sigma_k = 2, \sigma_\omega = 2$ and were implemented in the present work without any modification.

VOF Model

The Volume of Fluid (VOF) model was implemented to capture the interactions between various fluid phases – water, vapor, air, and liquid steel, especially as it is can predict the breakup of fluid due to surface tension effects.

Velocity and pressure were solved via the Navier-Stokes equation, a continuum momentum conservation equation for incompressible flow. The behavior between phases was tracked by solving the continuity equation for the volume fractions of one or more phases. The continuity equation used in VOF can be expressed as follows [12]:

$$\frac{1}{\rho_q}\left[\frac{\partial}{\partial t}\left(\alpha_q\rho_q\right) + \nabla\cdot\left(\alpha_q\rho_q\vec{v}_q\right)\right] = S_{\alpha_q}$$

where S_{α_q} is the mass source term which is zero unless defined otherwise.

The continuity equation does not solve for the volume fraction of the primary phase, instead, it is computed based on the following constraint [12]:

$$\sum_{q=1}^{n}\alpha_q = 1$$

Evaporation Model

The Lee model [13] [14] was used to investigate the possibility of vapor pocket formation at the molten metal/water jet interface. The general phase-change equation for evaporation can be written as follows:

$$\dot{m}_{vapor} = -\dot{m}_{liquid} = r\alpha_l\rho_l\frac{T-T_{sat}}{T_{sat}};\ T > T_{sat}$$

where r is a relaxation constant used to avoid divergence issues. α_l and ρ_l are the volume fraction and density of the water phase respectively.

2.2 Model Setup

Fig.2a) illustrates the geometrical configuration of the V-jet water atomizer used in the present investigation. An axisymmetric model was developed based on the area of interest of the water atomizer with V-jet nozzles, as shown in Fig.2b. The model was built axisymmetrically along the center of the molten metal stream due to the symmetrical configuration of the water atomizer. The primary nozzle is located at the top of the computational domain. The computational domain consists of about 100,000 quadrilateral cells. The grid is refined where the region having the fluid-fluid interactions are the most intense.

In this model, the inlet of the molten metal is simulated near the impingement point of water jet. A preliminary study showed the irregularity of the metal jet stream due to turbulent flow caused by the incoming water jet. Thus, the inlet was extended to minimize the effect the 2D model. The velocity of molten metal was also adjusted to 10m/s in order to compensate for the irregular behavior of molten metal flow in the turbulent zone created by water jet impingement. The molten metal temperature at the inlet was adjusted to 1900 K to account for the slight temperature drop during the free-falling stage. The water jet velocity was specified to be 140m/s, which is equivalent to ~10MPa. The outlet of the domain was set to have a static pressure of 1 atm. All solid walls were considered stationary and no slip. Fig.2c) shows the outline of the computational domain.

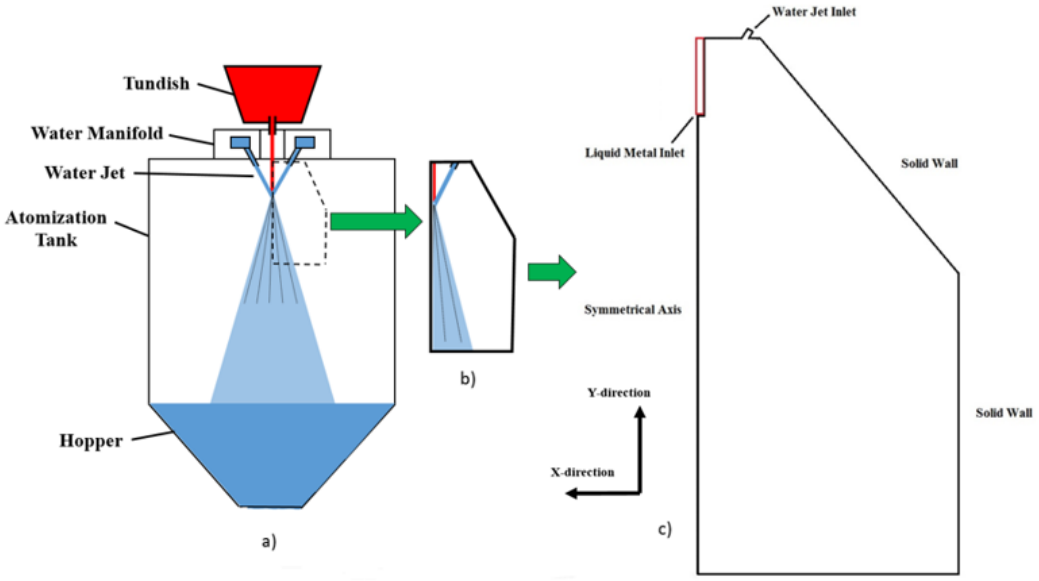

Figure 2. Configuration of (a) Water Atomization, (b) Area of Interest, (c) Computational Domain

The operational parameters used for this investigation are listed in Table 1, where D_M/D_0 is the ratio of molten metal nozzle diameter to the water jet nozzle diameter.

Table 1: Operational Parameters of Molten Steel.

Parameter	***Value***	***Units***
Density (ρ)	7000	kg/m^3
Surface Tension (γ)	1.6	N/m
Viscosity (μ) (at 1900 K)	3.93	mPa s
Ratio of Nozzle Diameters (D_M/D_0)	2	
Molten Metal Temperature	1900	K
Liquidus Temperature	1800	K
Solidus Temperature	1717.15	K
Latent Heat	272	kJ/kg

As operational parameters such as apex angles and surface tension were shown to influence the final particle size distribution in previous studies, they were investigated in the following six different cases, as listed in Table 2. The first four cases focus on the influence of the apex angle, while the last two cases examine the influence of the surface tension of molten metal.

Table 2: Summary of various cases examined.

Case	Water Jet velocity (m/s)	Liquid Steel velocity (m/s)	Apex angle (degree)	D_M/D_0	Surface tension (N/m)
1	140	10	15	2	1.6
2	140	10	20	2	1.6
3	140	10	25	2	1.6
4	140	10	30	2	1.6
5	140	10	20	2	1.2
6	140	10	20	2	0.9

Fig.3 defines the apex angle as the angle between the molten metal stream and the water jet.

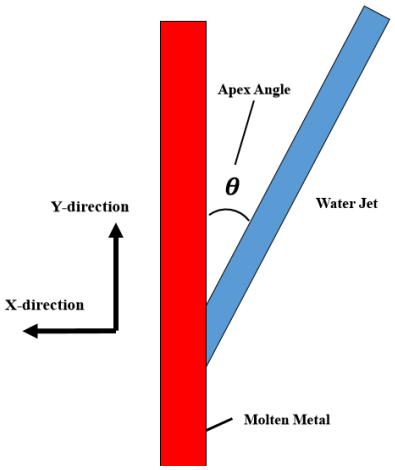

Figure 3. Illustration of apex angle.

Estimation of Dynamic Viscosity

In the present investigation, the change of molten metal viscosity is implemented into ANSYS Fluent using the mathematical model proposed by Hirai [15]. The model estimates the change of viscosity with respect to temperature from the operational temperature to the solidus temperature.

$$\mu = A \cdot \exp\left(\frac{B}{R \cdot T}\right)$$

$$A = \frac{(1.7\times10^{-7})\cdot\rho^{2/3}\cdot T_m^{1/2}\cdot M^{-1/6}}{exp[B/(R\cdot T_m)]}$$

$$B = 2.65 \cdot T_m^{1.27}$$

μ is the liquid metal viscosity, R is the ideal gas constant, ρ is the density of metal at room temperature, T is the temperature of molten metal, T_m is the liquidus temperature, and M is the atomic weight.

3. Results and Discussion

3.1 Flow Speed of the Water Jet with Respect to Apex Angle

Change of velocity components with respect to the apex angle significantly influences the atomization process since it determines the amount of momentum transferred from water jet to the molten metal stream. The velocity magnitude of water jet was measured at ~132 m/s for all apex angles at the moment prior to the impact with molten metal surface. The minor loss from initial jet velocity is likely due to the air drag and expansion of water jet. Calculating with trigonometric functions, the horizontal velocity of water jet increased with increasing apex angles. It ranged from 34 to 66 m/s at 15 and 30 degrees, respectively.

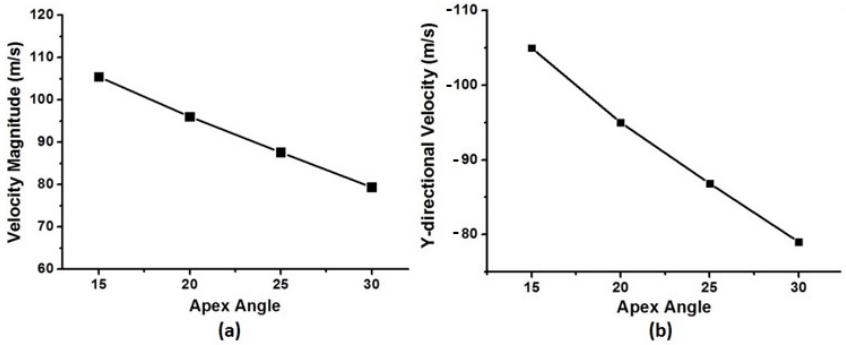

Figure 4. Variation of (a) Total velocity and (b) Y-directional velocity of water jets at the point of impact with change in apex angle.

At the point of impact with the molten metal surface, the total velocity of water jet decreased with increasing of apex angle, as shown in Fig. 4. Compared to the velocity prior to impact, the water jet lost about 20% of its total velocity at 15 degree and as much as 40% at 30 degree. It was found that for every 5-degree increase there is a ~9% decrease in the total velocity of the water jet. The decreasing trend of total velocity can be further examined through x-directional velocity at various apex angles. Measured at the surface of the molten metal for all inspected configurations, x-directional velocity dropped to approximately 8 m/s and there was minor loss in the y-direction. Although not explicitly measured, the water jet's x-directional velocity should eventually be decelerated to zero as it penetrates deeper into the molten metal stream. Therefore, it was observed that this collision caused a greater reduction in x-directional velocity, hence a larger horizontal momentum transfer from water jet to the molten metal, at higher apex angle was deduced.

The momentum transferred from water jet to molten metal over time is associated to the force inflicted to the molten metal surface. In water atomization, the force exerted onto the molten metal surface destabilizes the melt stream. As described by Dunkley [8], the normal impact of water jet onto a molten metal surface has more influence on the breakup of the molten metal stream. The shear force imposed by the water jet contributes to the thinning of the molten metal stream and results in Kelvin-Helmholtz (K-H) instability waves at the surface. Therefore, as observed in fig. 5, increasing apex angle results in higher horizontal force and causes molten metal to be destabilized and breaks up easily. While the same change in apex angle leads to less surface perturbation of the molten metal by vertical force, increased x-

directional force contributes toward fragmentation of the molten metal surface. Thus it is expected that increasing apex angle during primary atomization minimizes d_{50} of atomized metal.

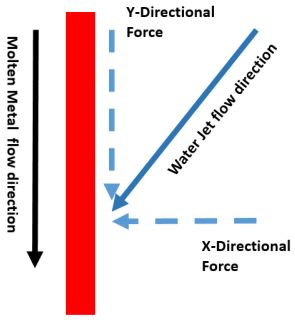

Figure 5. Illustration of force vector with respect to the molten metal flow.

Aligning with this expectation, previous investigators believe that increasing apex angle decreases the median particle size (d_{50}). However, it is important to emphasize the practical limitations of the nozzle configuration. As shown in Fig. 6, when apex angle increases, the distance between the impact point of the water jets and the inlet of molten metal flow decreases, which poses a risk of water splashing towards the nozzle opening. The splashing of water was also observed during 30^0 apex angle simulation. The phenomenon was also noted by Dunkley [8]. He stated that an apex angle greater than 50^0 is impractical in a water atomization setup as it would result in a significant amount of water splashing towards the tundish nozzle, leading to the solidification of molten metal at the tundish nozzle opening.

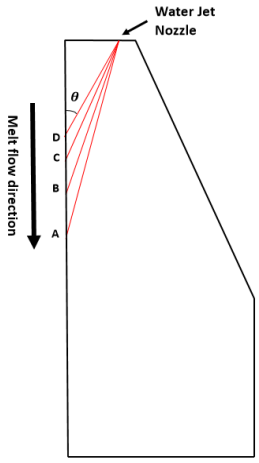

Figure 6. Illustration of impact locations with respect to apex angle: A = 15^0, B = 20^0, C = 25^0 and D = 30^0.

3.2 Kinetic Energy Transfer during Atomization

Fig. 7 shows the percentage kinetic energy loss of the water jet due to impact with the molten metal stream at various apex angles. It can be observed that, upon collision, the water jet loses about 70% of its initial kinetic energy ($E_{k,water\ jet}$), and total kinetic energy loss increases with apex angle. In comparison with the apex angle of 20^0, the loss of kinetic energy increases by ~2% at 25^0 and by ~5% at 30^0 whereas

decreases by ~0.9% at 15^0. Additionally, increasing the x-directional velocity also leads to increased kinetic energy transfer to the molten metal surface, as shown in Fig. 7. Kinetic energy acts as a factor to increase the instability of the molten metal surface.

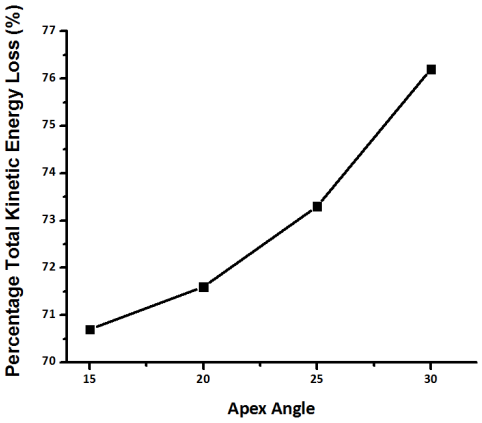

Figure 7. Percentage total kinetic energy loss due to the impact of water jet with molten metal.

The kinetic energy per unit length of the water jet before and during the impact is measured using the following equation:

$$E_k = \iint \frac{1}{2}\rho \cdot v^2 \cdot dxdy$$

$$E_{k,loss} = E_{k,waterjet} - E_{k,after\ impact}$$

where ρ is the density of water, v is the velocity magnitude of the water jet, and $E_{k,after\ impact}$ is the kinetic energy of water jet immediately after impacting molten metal surface.

Ashgriz [16] describes that kinetic energy is the driving force for atomization process. The kinetic energy transferring from the water jet to the molten metal results in the creation of a large amount of surface area. The kinetic energy is partially dissipated due to the resistance forces generated by viscous effects and the surface energy of the molten metal. From the energy conservation point of view, most kinetic energy added to the system will eventually transfer into surface energy, while a small amount is dissipated by viscosity. Energy conservation in atomization can be expressed by the following simplified equation [16]:

$$E_{k,i} + E_{s,i} = E_{k,f} + E_{s,f} + E_{diss}$$

where $E_k\ and\ E_s$ are the kinetic energy and surface energy, respectively; E_{diss} is the energy dissipated due to viscous effects of molten metal viscosity; subscripts *i* and *f* represent the initial and final states of the system, respectively.

With an increase of kinetic energy transfer from the water jet to the molten metal stream, the other terms in the equation, i.e. surface energy and dissipated energy, also increase to achieve equilibrium. The cumulative surface tension energy of the liquid metal increases due to the cascading breakup process and rapid growth of total surface area. Upon attainment of an equilibrium state, the kinetic energy that is transferred to the liquid metal phase can no longer overcome the surface energy. Thus, the breakup of the liquid metal droplets reaches its limit.

3.3 Influence of Surface Tension

As mentioned in a previous section, surface tension is a factor opposing the disintegration of the molten metal stream. To account for the effect of surface tension on the breakup of a liquid, the Weber number (We) has been implemented into many mathematical analyses of droplet breakup and particle formation. The Weber number is a measure of disruptive inertial forces with respect to the stabilizing interfacial force of a liquid [17], as follows:

$$We = \frac{External\ Inertial\ Force}{Surface\ Tension} = \frac{\rho \cdot U^2 \cdot D}{\sigma}$$

A series of simple mathematical calculations were carried out to examine the possible degree of influence of the surface tension on the breakup of molten metal, addressing specifically at primary and secondary atomization zones. Primary atomization zone is the region of water jet and molten metal stream impingement. Secondary atomization zone is located immediately below the primary atomization zone where droplet collisions occur.

During primary atomization, the surface of molten metal stream is disrupted by the force of water jet in horizontal directions. Thus, the Weber number equation of molten metal stream in primary atomization zone can be written as follow:

$$We_{Stream} = \frac{\rho_{water} \cdot U_{rel,stream}^2 \cdot D_{melt\ stream}}{\sigma}$$

where $U_{rel,stream}$ is the relative velocity of water jet to molten metal stream in the horizontal direction.

Upon entering secondary atomization zone, the molten metal will have a much smaller characteristic length. In the calculation of the Weber number of a melt droplet, the melt was assumed to break into small droplets with diameter of 0.1 mm.

$$We_{Droplet} = \frac{\rho_{water} \cdot U_{rel,droplet}^2 \cdot D_{melt\ droplet}}{\sigma}$$

where $U_{rel,stream}$ is the relative velocity of water jet to molten metal droplet in the vertical direction.

Table 3: Calculated Weber numbers for the melt stream and for a melt droplet for various value of surface tension

Case	Surface Tension	We_{Stream}	$We_{Droplet}$
2	1.6	55026	623
5	1.2	73368	831
6	0.9	97824	1109

It was found from the calculation that the Weber numbers of primary atomization in this study are higher than were proposed by other researchers for the breakup of droplets [18, 19]. The differences may be explained through recognizing the diameters of droplets used in Lubarsky [18] and Li's [19] studies being in the range of several micrometers, which were smaller in magnitude by nearly an order of two than what was used here to calculate We_{Stream}. In this comparison, it can be seen that the diameter of the molten metal plays a significant role in determining the resulting value of the Weber number. This results in a significantly large numerator in the Weber number equation, which diminishes the influence of the

surface tension on the formation of droplets as shown in Table 3. On the other hand, during secondary atomization, the droplet diameter is ~100 times less than melt stream diameter. Therefore, the surface tension force starts to dominate during secondary atomization.

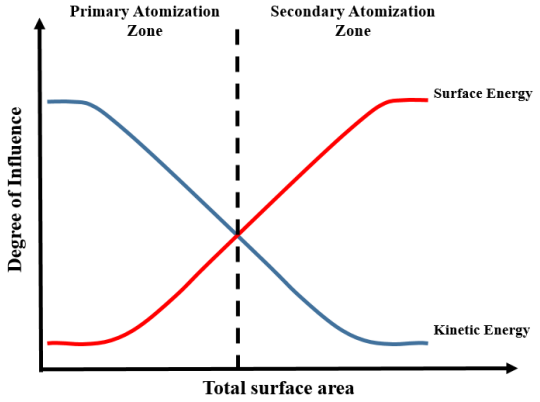

Figure 8. The degree of influence of kinetic energy and surface energy at various stages of atomization.

As illustrated in Fig. 8, it can be concluded that the breakup behavior of the molten metal in primary atomization is dominated by transfer of kinetic energy from water jet to melt stream. Surface tension has a minimal effect due to the domination of the external inertial force. The results from cases number 2, 5, and 6 shown in Fig. 9, agree with the finding from the mathematical calculations. The decrease of surface tension does not show a major influence on the change of molten metal behavior or increase in the formation of droplets in primary atomization zone.

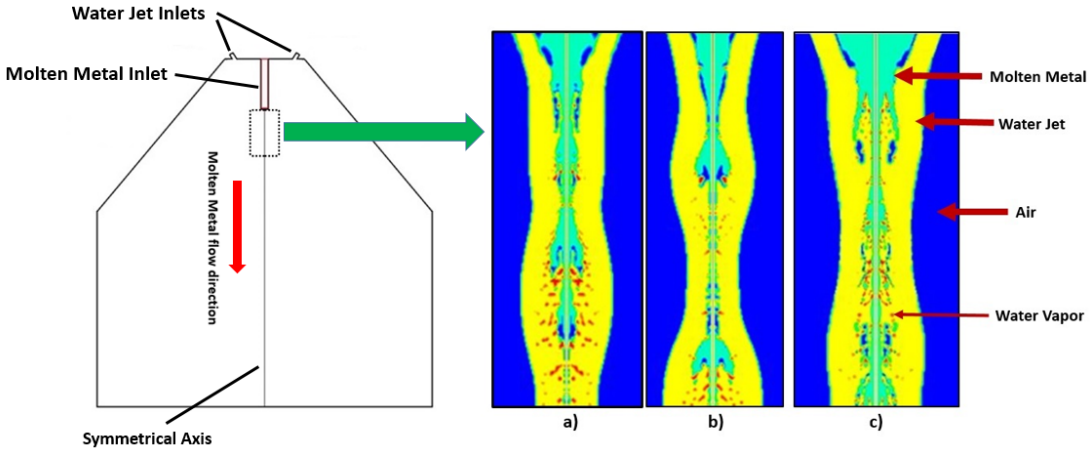

Figure 9. Phase contours at various surface tensions of a) 0.9, b) 1.2 and c) 1.6 N/m. Green indicates molten metal phase, yellow indicates water phase, blue indicates air phase and red indicates water vapor phase.

3.4 Formation of Water Vapor Leading to Vapor Explosion

Figure 10 illustrates that steam pockets form at the molten metal/water jet interface. It is known that the formation of steam pockets is one of the breakup modes for molten metal atomization, which assists the formation of droplets from the molten metal surface. The results of this study show that the momentum of the water jet entrenches the steam pockets into the molten metal stream further, thereby detaching the

developing surface portion from the main stream. The entrenched steam pockets increase the instability of molten metal surface, which accelerates the formation of molten metal droplets. The present result is similar to Aller's illustration of formation of steam pockets [10]. In addition, our result shows that in the downstream, some steam pockets assist in the formation of metal droplets on the surface of the molten metal stream.

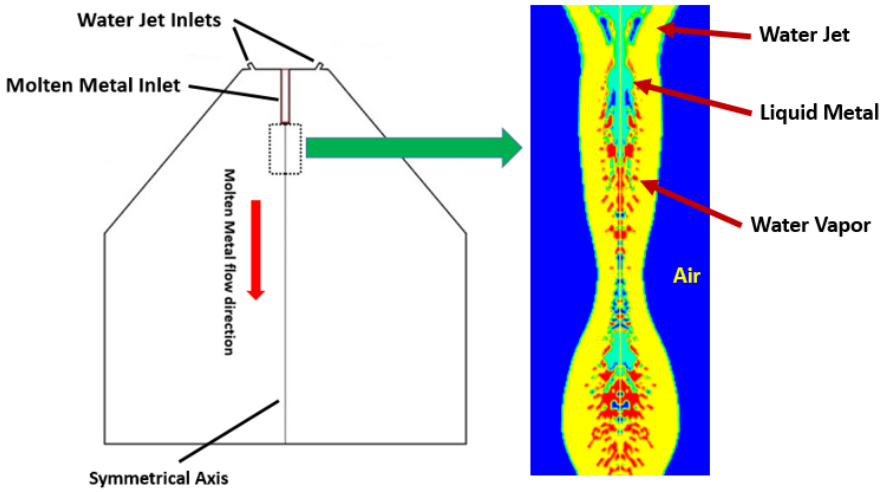

Figure 10. Phase contours of fluid flow with apex angle of 20 degrees. Green indicates molten metal phase, yellow indicates water phase, blue indicates air phase and red indicates water vapor phase.

The formation of steam pockets may further lead to behavior similar to a vapor explosion. Vapor explosion is a process of intense heat transfer between the fuel (molten metal) and the coolant (water jet), resulting in the rapid formation of water vapor/steam at the molten metal/water interface. As described by Iida [20], during the initial contact of hot and cold liquids, a thin vapor film forms at the molten metal/water jet interface creating a stable barrier. However, the barrier can be easily destabilized by water jet impact, thermal film destabilization or water entrapment within the molten metal [21]. The destabilization of barrier leads to direct liquid-liquid contacts, thus causing more vapor formation and rapid vapor expansion at molten metal/waterjet interface. As the result of such explosive phenomenon, the molten metal breaks up into smaller fragments.

It has been found that such phenomena can occur within milliseconds for metal alloys with low melting points (600~800°C) [22]. In the present investigation, the molten metal has a temperature of 1600°C. Thus, it can be expected that water will evaporate much faster, allowing rapid formation of steam pockets on the surface of the molten metal stream. Since the explosion behavior model was not implemented in this CFD study, the molten metal stream was broken by momentum and shear forces generated by the collision with the water jet. However, it can be concluded that the extreme temperature difference at the molten metal/water jet interface fuels the rapid formation of steam pockets. This results in a violent chain reaction of vapor explosion. Therefore, it is suspected that vapor explosion may partly contribute to the significant disintegration of molten metal.

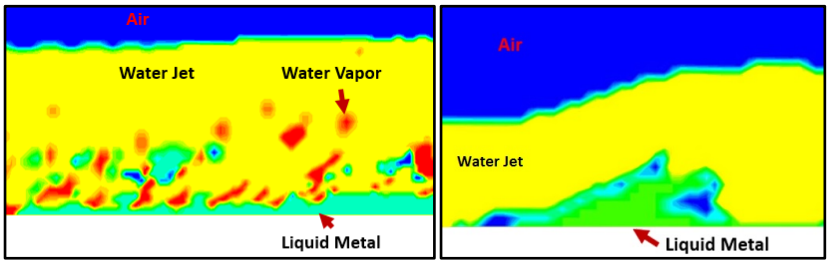

Figure 11. Comparison of the molten metal and water jet interface with the consideration of water evaporation (Left) and without evaporation (Right).

In this investigation, a validation test was used to show the difference between cases when the formation of water vapor was considered, and when it was neglected. As shown in Fig. 11, it can be seen that the simulation without evaporation model has a uniform surface compared to the one with evaporation model.

4. Conclusion:

The interaction between a molten metal stream and a water jet during primary atomization was studied by using CFD techniques. The influence of the primary nozzle apex angle and molten metal surface tension on the behavior of molten metal stream was reported. A higher apex angle ensures more energy transfer into the metal stream and can help in creating smaller droplets in the primary atomization zone. Surface tension is believed to have a minimal effect in the primary region because of higher inertial forces and larger length scales. The formation of water vapor at the molten metal stream/water jet interface was successfully visualized. Further studies will focus on the following aspects: Implementation of a 3D computational domain to study primary atomization; Involvement of secondary atomization by implementing secondary nozzles; Visualization of the breakup of molten droplets in secondary atomization.

Acknowledgements:

The authors would like to thank Rio Tinto Fer et Titane and especially the technology center and powder plant personnel for their support of this study.

Nomenclature:

γ_k	effective diffusion for turbulence kinetic energy	μ	viscosity [mPa s]
γ_ω	effective diffusion for specific dissipation rate	T_m	liquidus temperature [K]
k	turbulence kinetic energy	R	gas constant [j/K mol]
ω	specific dissipation rate	M	atomic weight [kg/mol]
G_k	production of turbulent kinetic energy	E_k	kinetic energy [J]
G_ω	production of specific dissipation rate	E_s	surface energy [J]
Y_k	dissipation of turbulence kinetic energy	E_{diss}	dissipated energy [J]
Y_ω	dissipation of specific dissipation rate	σ	surface tension [N/m]

S_k	user-defined source term for turbulence kinetic energy equation	We	weber number, $\rho \cdot U^2 \cdot D/\sigma$
S_ω	user-defined source term for specific dissipation rate equation	We_{Stream}	weber number of molten metal stream, $\rho \cdot U_{stream}^2 \cdot D/\sigma$
μ_t	turbulent viscosity	$We_{Droplet}$	weber number of molten metal droplet, $\rho \cdot U_{droplet}^2 \cdot D/\sigma$
α	coefficient defined to be equal to 1 in a system with high-Reynolds number	U_{rel}	relative velocity between molten metal stream and water jet [m/s]
$\vec{v}$	vector velocity [m/s]	$D_{melt\ stream}$	diameter of molten metal stream [m]
S_α	source term	$D_{melt\ droplet}$	diameter of molten metal droplet [m]
ρ	density [kg/m^3]		
$\vec{v}$	fluid velocity [m/s]	**Subscript:**	
$\dot{m}_{vapor}$	Interfacial mass transfer flux of vapor [kg/m^3 s]	q	primary phase
$\dot{m}_{liquid}$	Interfacial mass transfer flux of liquid [kg/m^3 s]	$k, loss$	kinetic loss
r	mass transfer intensity factor [1/s]	$k, water\ jet$	kinetic of water jet
α_l	volume fraction of liquid phase	$k, after\ impact$	kinetic after impact
T	temperature [K]	l	liquid phase
T_{sat}	saturated temperature [K]	i	initial state
D_M/D_0	ratio of nozzle diameters	f	final state

Reference:

[1] J. Dunkley, "Blown to atoms: How to make metal powders," *Met. Powder Rep.*, 2002, vol. 57, no. 11, pp. 18–19.

[2] F. Persson, A. Eliasson, and P. Jönsson, "Prediction of particle size for water atomized metal powders," *Powder Metall.*, 2012, vol. 55, no. 1, pp. 45–53.

[3] J. J. Dunkley and J. D. Palmer, "Factors Affecting Particle Size of Atomized Metal Powders," *Powder Metall.*, 1986, vol. 29, no. 4, pp. 287–290.

[4] B. Bergquist and T. Ericsson, "A Robustness Simulation of Water Atomization," *Powder Metall.*, 2000, vol. 43, no. 1, pp. 37–42.

[5] B. Bergquist, "New Insights into Influencing Variables of Water Atomisation of Iron," *Powder Metall.*, 1999, vol. 42, no. 4, pp. 331–343.

[6] F. Persson, "A Study of Factors Affecting the Particle Size for Water Atomised Metal Powders." Division of Applied Process Metallurgy, Department of Material Science and Engineering, School of Industrial Engineering and Management, 2012, Licentiate Thesis, Royal Institute of Technology, KTH, Stockholm, Sweden.

[7] N. B. Dhokey, M. G. Walunj, and U. C. Chaudhari, "Influence of water pressure and apex angle

on prediction of particle size for atomization of copper powder," *Adv. Powder Technol.*, 2014, vol. 25, no. 2, pp. 795–800.

[8] J. J. Dunkley, "Atomization", *ASM Handbok*, edited by P.W. Lee, Y. Trudel, R. Iacocca, R.M. German, B.L. Ferguson, W.B. Eisen, K. Moyer, D. Madan, and H. Sanderow, ASM International, 1998, vol. 7, part 6, pp. 35-52.

[9] R. J. Grandzol and J. A. Tallmadge, "Water Jet Atomization of Molten Steel," *AIChE J.*, 1973, vol. 19, no. 6, pp. 1149–1158.

[10] A. J. Aller and A. Losada, "Models in Metal Powder Atomization," *Powder Met. Sci. Technol.*, 1991, vol. 2, no. 2, p. 13.

[11] D.C. Wilcox, *Turbulence Modeling for CFD*, 1993, DCW Industries, Inc., La Cañada, CA.

[12] Southpointe, *ANSYS-Fluent 15.0 Theory Guide*, 2013, ANSYS Inc, Canonsburg, PA.

[13] W.H. Lee, "A Pressure Iteration Scheme for Two-Phase Flow Modeling", *Multiphase transport: Fundamentals, Reactor Safety, Applications*, Hemisphere Publishing, Washington, DC,1980, vol. 1, pp. 407-431.

[14] D. Sun, J. Xu, and Q. Chen, "Modeling of the Evaporation and Condensation Phase-Change Problems with FLUENT," *Numer. Heat Transf. Part B Fundam.,* 2014, vol. 66, no. 4, pp. 326–342.

[15] M. Hirai, "Estimation of viscosities of liquid alloys," *ISIJ Int.*, 1993, vol. 33, no. 2, pp. 251–258.

[16] A. Ashgriz, *Handbook of Atomization and Sprays*, 2011, Springer.

[17] Li. D, "Weber Number", *Encyclopedia of Microfluidics and Nanofluidics*, Springer, Boston, MA, 2008, pp.2185.

[18] E. Lubarsky, J. R. Reichel, B. T. Zinn, and R. McAmis, "Spray in Crossflow: Dependence on Weber Number," *J. Eng. Gas Turbines Power*, 2010, vol. 132, no. 2, pp. 021501-1 - 021501-9.

[19] X. Gang Li and U. Fritsching, "Process modeling pressure-swirl-gas-atomization for metal powder production," *J. Mater. Process. Technol.*, 2017, vol. 239, pp. 1–17.

[20] Y. Iida, T. Takashima and R. Akiyoshi, "A Study of the Vapor Explosion Mechanism with Single Drops of High-Temperature Liquids and Volatile Liquids," *JSME International Journal,* 1987, vol. 30, no. 270, pp. 1972-1981.

[21] G. Berthoud, "VAPOR EXPLOSIONS," *Annu. Rev. Fluid Mech*, 2000, vol. 32, pp. 573-611.

[22] K. H. Bang, J. M. Kim and D. H. Kim, "Experimental Study of Melt Jet Breakup in Water," *Journal of Nuclear Science and Technology*, 2003, vol. 40, no. 10, pp. 807-813.